International Journal of Mass Spectrometry 309 (2012) 176–181

Contents lists available at SciVerse ScienceDirect

International Journal of Mass Spectrometry

journal homepage: www.elsevier.com/locate/ijms

Growth kinetics of Al clusters in the gas phase produced by a magnetron-sputtering source

Zhixun Luo[a], W. Hunter Woodward[a], Jordan C. Smith[a], A.W. Castleman Jr.[a,b,*]

[a] Department of Chemistry, Pennsylvania State University, University Park, PA 16802, United States
[b] Department of Physics, Pennsylvania State University, University Park, PA 16802, United States

ARTICLE INFO

Article history:
Received 1 May 2011
Received in revised form
22 September 2011
Accepted 22 September 2011
Available online 1 October 2011

Keywords:
Metallic clusters
Size-controllability
Magnetron-sputtering
Cluster growth

ABSTRACT

A magnetron-sputtering (MagS) cluster source was used to produce metal clusters of different size distributions by varying individual source parameters. Selectivity of the size of the Al clusters was observed and the mass distribution presents wide-range controllability by the MagS-source, which enables experimental determination of the growth process of Al clusters. By implementing the extended Smoluchowski rate equation, here we propose an interpretation of the cluster-growth kinetics in the gas phase environment. A collision-dependent growing time domain is demonstrated.

1. Introduction

Cluster formation processes are typically very fast; hence it is difficult to directly observe the initial real-time growing process [1–7]. In this regard, despite tremendous advancements in cluster science, the underlying mechanistic processes leading to micro-scale assembly, crystal formation, and cluster growth have not been fully explored [8–11]. Recent advances in cluster science have inspired considerable interest in the fundamental principles of cluster growth [12–16]. A better understanding of the growth kinetics of all-metal clusters, which have demonstrated advantageous properties for use in catalysts and cluster-assembled materials, would greatly expedite the eventual large-scale use of these sub-nanoscale materials.

In the case of clusters deposited onto a solid substrate [17–20], the growth processes can be investigated via high-resolution microscopy to monitor the early stages of the phenomenon [21,22]; additionally, the growth mechanism of liquid clusters can be identified using the Wolde–Frenkenl cluster definition [23,24]. However, although growing processes may be observed in these examples, the size-regime of clusters makes it difficult to monitor the initial stage. A number of subtle questions regarding the growth of clusters remain undetermined and are still debated due to a lack of evidence on how burgeoning clusters initially begin to grow.

Indirectly observing the growth kinetics of gas-phase clusters may provide useful information in the fields of surface, liquid, and gas-phase nanomaterials. Because of the difficulty in a direct approach, a controllable source that provides uniform distributions of the target atoms or small clusters is an important precondition [25]. Among the several available sources at present, most utilize the vaporization of a metal in a relatively high pressure volume and a subsequent expansion into a low pressure volume [26–37]. However, the ability to produce different cluster distributions is limited in almost all of these techniques due to a source that is non-modifiable without interrupting the experiment. This creates a cluster distribution that is almost entirely fixed. Alternatively, a cluster distribution can be obtained by employing a magnetron sputtering technique which has been widely utilized to perform atomic layer deposition and produce thin film materials [38–44]. The appeal of this source in the current study is that it operates under several variable parameters that affect the cluster distribution in some way, and thus allows one to indirectly observe the influences that affect cluster growth. Herein, we employ a magnetron-sputtering (MagS) cluster source to investigate the growth kinetics of gas-phase clusters. Variable size distributions were observed and several parameters of the MagS-source system affecting the mass distributions were identified. These parameters produce distributions which mimic the theoretical modeling results based on the extended Smoluchowski rate equation [45,46]. Such experimental and theoretical investigations provide detailed

---

* Corresponding author at: Department of Chemistry, Pennsylvania State University, 309 Chemistry Building, University Park, PA 16802, United States.
Tel.: +1 814 865 7242; fax: +1 814 865 5235.
E-mail address: awc@psu.edu (A.W. Castleman Jr.).

1387-3806/$ – see front matter © 2011 Elsevier B.V. All rights reserved.
doi:10.1016/j.ijms.2011.09.016

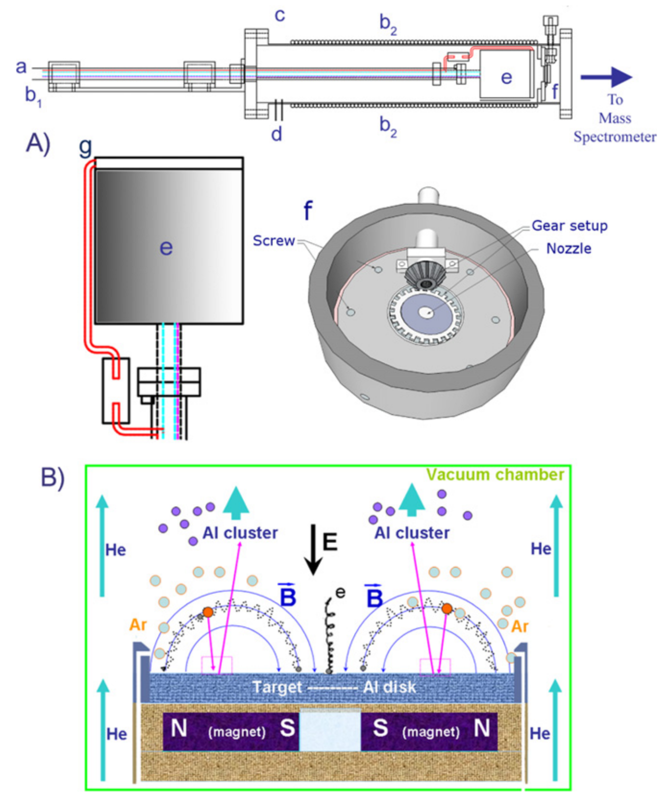

Fig. 1. (A) Sketch of the experimental set-up for production and analysis of the size-controlled clusters. Some of the components are labeled: (a) inlet of Ar and electric wire; (b) inlet of cooling water; (c) magnetron axial mount and the shell of vacuum chamber with cooling water; (d) inlet of He; (e) magnetron head with target; (f) nozzle; (g) outlet of Ar; (B) mechanism sketch of the MagS-source, corresponding to the enlarged part of the magnetron head.

knowledge at some extent about the growth kinetics of clusters in their initial states.

2. Experimental

The fast-flow tube apparatus employed in the experiment followed the corresponding designs detailed in previous studies [47,48]. A graphic illustration depicting the improvements on this system for the present work is shown in Fig. 1. Clusters formed in front of the magnetron head flow through a nozzle (f), then into the flow tube and to be analyzed by the mass spectrometer. The extraction region and mass spectrometer is described in detail elsewhere [49].

The DC-compatible magnetron system was designed based on a circular TORUS® magnetron sputter source (Kurt J. Lesker Company). The cooling water used to prevent overheating both inside the head and around the vacuum chamber was maintained at 10 °C at a flow rate of 2.8 LPM. The Ar gas (1–15 mTorr, High Purity, Praxiar, Inc.) was introduced through the inner pipeline (a) to maximize concentration at the front of the source. A magnetron axial mount (c) enabled the whole magnetron head to move back and forth in the chamber without breaking vacuum, and was sealed with an o-ring compression fitting (Ultra-Torr, Swagelok). Helium (0.8–3 Torr, High Purity, Praxiar, Inc.) was introduced from the inlet (d) at the rear, to carry the clusters through an iris of adjustable diameter which worked as the outlet for the clusters into the mass spectrometer. A 1.6 kW DC power supply (Power Supply Make/Model) was used to provide the high voltages needed for the magnetron sputtering.

The Al target (no purity rating, disk-shaped, Φ50-mm, and 6-mm thickness) was fixed onto the magnetron head before placing it the vacuum chamber. The gap between the dark space shield and the grounded sides of the head was approximately 2 mm, and was designed and built after considering the Paschen curve for Ar and stainless steel and the pressures and voltages to be used [50]. When operating the magnetron system, the power supply voltage was first increased until the power supply registered a current reading (−240 V to −260 V), before adjusting the various parameters to achieve the desired cluster distribution. These parameters, as described above, include (1) the flow/partial pressure of Ar; (2) the flow/partial pressure of He; (3) the distance between the magnetron head and the exit iris; (4) the diameter of the iris; and (5) the voltage/current of the power supply. Although not covered in this study, another optional parameter involves the temperature of the cooling system, which would affect the collision rates and energies of the species in the source.

3. Results and discussion

Fig. 2 presents two mass spectra of Al clusters obtained by the MagS-source. The two spectra seem to suggest a normal size distribution (Gaussian profile) of the formed Al clusters, centered at Al_6/Al_7 (Fig. 2a) and $Al_{32–44}$ (Fig. 2b), depicted by the dotted line Gaussian fit. The size selectivity in Fig. 2 results solely from adjustments in the parameters of the MagS-source [40] suggesting a tunable size distribution of the obtained Al clusters. It is important to mention that the partial pressure of Ar and the distance between

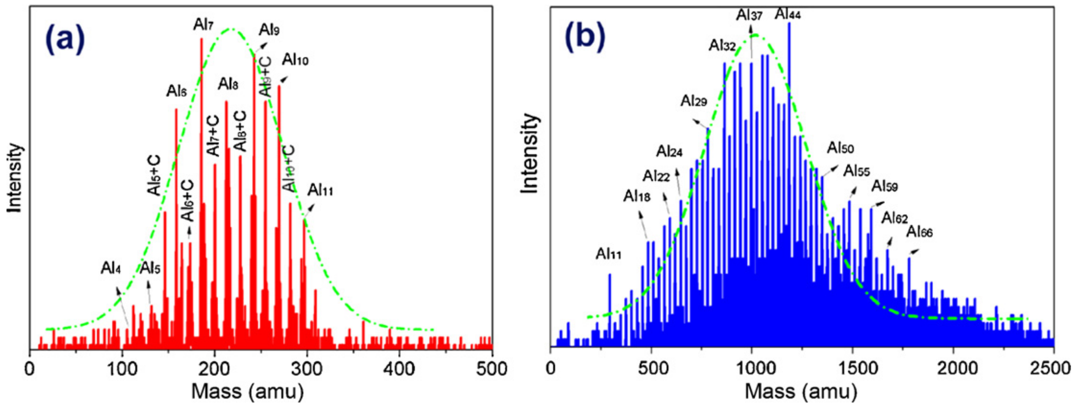

Fig. 2. Al clusters obtained by MagS-source system: (a) collected with He and Ar pressures in the magnetron chamber at 2 Torr, pressure in the flow tube is 0.51 Torr; the distance target from nozzle is at 90 mm, voltage at 243.3 V; (b) collected with He and Ar pressures at 2 Torr, pressure in the flow tube is 0.51 Torr, the distance at 130 mm, voltage at 255.9 V.

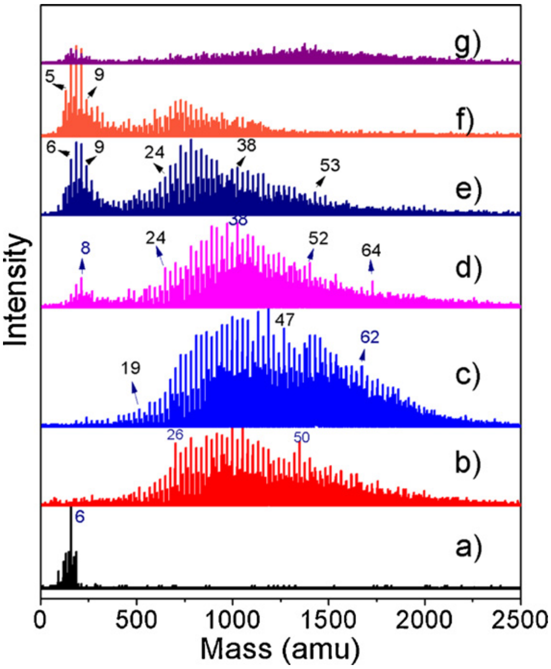

Fig. 3. Al clusters produced by magnetron source at different Ar pressures: with the magnetron pressures (Ar + He) at: 1.4, 1.6, 1.8, 2.0, 2.2, 2.4, 3 Torr, respectively. The intensities in the mass spectra refer to offset values, respectively. All spectra were collected at the same He pressures, the same cathode voltage (257.2 V), and the same distance (128.9 mm). All spectra were taken using the same lens setting, quadrupole bias and parameters of the mass analyzer.

the source head and the exit iris play the most important roles in determining the size distribution, as has been previously observed [51]. It is also worth mentioning that the He gas not only works as a carrier to transport the Al clusters through the fast flow tube, but also functions to cool the energetic Al atoms and clusters ablated from the target, via collisions with the source's inner walls [52].

Fig. 3 shows several mass spectra collected under different pressures of Ar. When small quantities of Ar were employed, very small Al clusters were obtained (Al_{4-11}) with the distribution centered at Al_6 (Fig. 3a); however, a completely different Al cluster distribution was observed when the Ar pressures increased (Fig. 3b and c). This change results from the growth of Al clusters being dependent upon the inelastic collisions which increase under higher Ar pressures. Further increasing the Ar pressure, both the small and large Al clusters can be observed simultaneously. This indicates that, due to the increased pressure-difference between the magnetron and flow-tube, some of the small clusters do not have sufficient time to accumulate before they travel into the flow tube. On the other hand, too much Ar will decrease the sputtering efficiency (Fig. 3g). These observations are supported by past studies under similar conditions [51].

Previously, however, it was implied that the voltage of the source does little more than to increase or decrease the overall intensity of the clusters. In the source, Ar^+ ions, which work as the sputtering substance, are accelerated by a high voltage applied to the target. The voltage on the target not only accelerates attracted Ar^+ ions into the target, but also provides abundant electrons which collide with Ar atoms to ionize additional Ar atoms (described as $Ar + e^- \rightarrow Ar^+ + 2e^-$). Hence the voltage must be high enough to overcome the threshold value and maintain sputtering efficiency; but after sustained plasma is born, increasing voltage/current will only result in more violent sputtering and subsequently more clusters. Fig. 4 shows the size distributions of Al clusters created by the MagS-source with voltages of −240 V, −250 V, −257.2 V, and −259.5 V, respectively (all other parameters were constant). The small clusters found at −240 V (a) were not observed with a negative voltage of −257.2 V or −259.5 V; instead, a distribution of larger clusters was obtained. Both the smaller and larger Al clusters coexist in the spectrum at −250 V, as shown in Fig. 4b, which is similar to observations made in past studies using high partial pressures of Ar [51]. As addressed below, it is possible that this increase in average mass was due to the contributions from the increased quantity of electrons in the limited space above the target surface.

Additionally, the diameter of the exit iris and its distance from the target were examined. As the gasses were controlled via needle valves, the diameter of the iris is directly proportional to the partial pressure of Ar and in the quantity of Al clusters obtained;

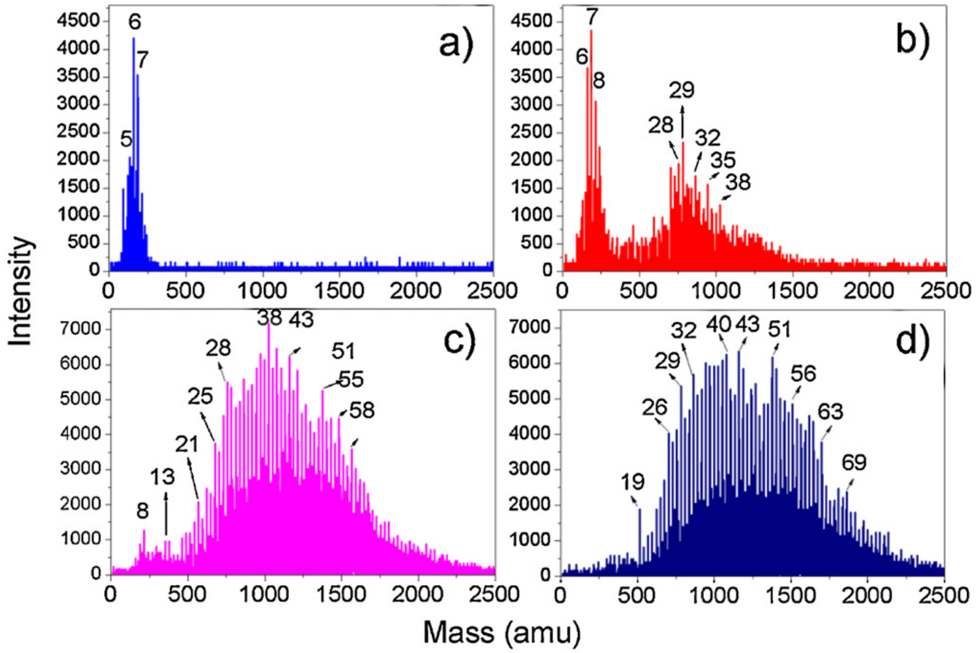

Fig. 4. Al clusters produced by the MagS-source at different voltages. All spectra were collected at the same He and Ar pressures (2 Torr), the same distance (128.9 mm). All spectra were taken using the same lens setting, quadrupole bias and parameters of the mass analyzer.

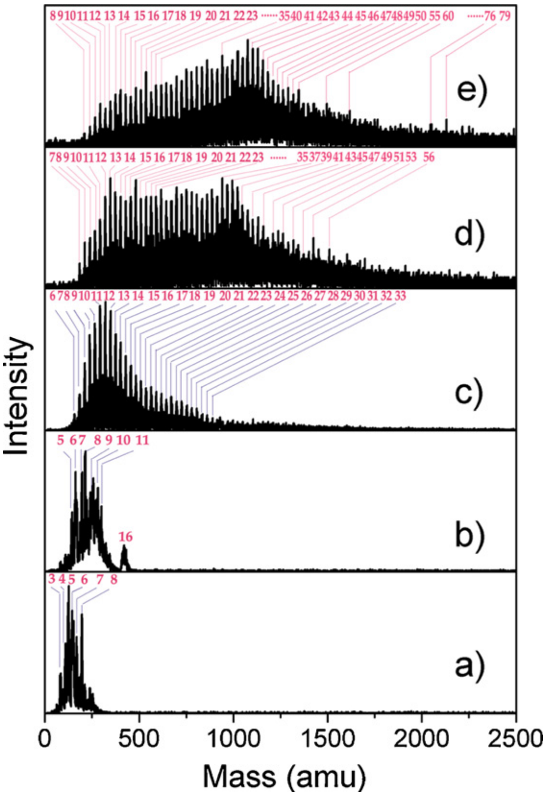

Fig. 5. Al clusters produced by MagS-source at different distances: 89 mm, 108 mm, 128 mm, 149 mm, 169 mm, respectively. All spectra were collected at the same He and Ar pressures (2 Torr), the same cathode voltage (257.2 V). All spectra were taken using the same lens setting, quadrupole bias and parameters of the mass analyzer.

however, the size distribution of Al clusters is highly sensitive to changes in the distance between the head and the nozzle, which is in good agreement with previous studies [51]. Smaller Al clusters were obtained at short distances, as shown by Fig. 5a; while larger clusters result from longer distances (Fig. 5a–e). In addition, a saturation effect (maximum size) was observed past a specific distance, while a very weak mass signal was obtained (low intensity) if the distance was too short. The information discussed above is summarized in Table 1, which presents a series of experimental parameters that all yield the same mass distribution and intensity. It can be seen that all of the described tunable parameters are responsible for the formation of clusters of varying size, and not just the distance between the head and the exit and the partial pressure of Ar. It is also seen that the MagS-source is capable of adjusting all of these parameters in order to achieve the desired mass distribution, which is a strong argument for its use over other all-metal cluster sources used in gas-phase or deposition studies.

In the past, the formation of a cluster distribution has been attributed to the "aggregation time," which quite simply is related to the number density of the metal atoms and the time before they are expanded into the vacuum apparatus. The aggregation time of Al clusters in the MagS-source is not only determined by the space immediately between the target and the exit of the source, but also dependent on the instantaneous pressures in the "waiting room" [26,37]. The initial formation of a dimer is directly related to the quantity of inert gas (Ar in the current example, due to its high polarizability when compared with He), as it requires a three-body collision wherein two metal atoms collide with an Ar atom, allowing the Ar atom to leave with enough kinetic energy that the resulting dimer does not spontaneously dissociate. In order to give further interpretation on principles of statistical mechanics, we refer to kinetics theories proposed previously [14–16,23,53]. Here, we explore these kinetics further by way of the Smoluchowski rate equation [45,46] which was originally used to describe the irreversible aggregation process of small particles and has been extended to describe the formation kinetics of clusters in the gas phase [54]. This assumes formation of a neutral Al_n distribution and an anionic Al_n^- distribution, expressed by the following reaction:

$$Al_m + Al_{n-m} \rightarrow Al_n; \quad Al_m^- + Al_{n-m} \rightarrow Al_n^- \tag{1}$$

The extended Smoluchowski rate equation can then be described as follows [54]:

$$\frac{dp_n}{dt} = \frac{1}{2}K\sum_{i+j=n} p_i p_j - K\sum_{i=1}^{\infty} p_n p_i - K'\sum_{i=1}^{\infty} p_n q_i \tag{2}$$

$$\frac{dq_n}{dt} = K'\sum_{i=1}^{n} q_i p_{n-i} - K' q_n \sum_{i=1}^{\infty} p_i \tag{3}$$

where p_n and q_n are the number of the neutral Al clusters and cluster ions of size n, respectively, and K and K' are the rate constants in the above formation reactions. Consequently, an analytical solution to the above equation is:

$$q_1 = q_0 \frac{1}{(1+u)^a}; \quad q_n = q_0 \frac{\prod(a+i-2)}{(n-1)!} \frac{u^{n-1}}{(1+u)^{a+n-1}} \tag{4}$$

It is seen that the relationship is similar, but not identical to, the inverse gamma distribution. Here, $a = 2K'/K$ and $u = 1/2Kp_0t$, q_0 and p_0 refer to constants uncorrelated to q_n or p_n. With several couples of different values of u and a, the calculated size distribution curves are shown as in Fig. 6. When the parameters are defined, the function can take on a curve which closely resembles the size distribution of the clusters observed in Fig. 5. Further, the most probable value of the cluster size can be calculated from $dq_n/dn = 0$. A result based on approximated simplification can be evaluated as $n_{max} = u\,(a-1)$, which accords with the experimental observations presented here. This suggests that the experimental parameters are related to the variables in the above equation. For instance, cathode voltages (V) and Ar pressures (P_{Ar}) (in the MagS-source) can be assigned to a variation of the a-value in Eq. (4), as described as $a \propto F(V, P_{Ar})$; On the other hand, the growing time domain (e.g., distance of target surface from the nozzle) can be considered as correspondence to the t in u-value in Eq.(4), depicted as $u \propto 1/2Kp_0d$, assuming the flowing velocity of Al clusters to be constant in the case of a steady condition. Other variables in general theory of crystal growth, such as monomer concentration and saturation, etc,

Table 1
A list of the parameters to reach an identical mass distribution of Al clusters in this work.

U (V)	I (A)	d (mm)	D (mm)	P_1 (Torr)	P_2 (Torr)	ν (Nm^3/h)
240–260	0.4–1.5	128	10	2.2	0.5	6.5
243.3	1.089–1.3	89–170	10	2	0.51	6.5
255.8	1.21	128	2–10	0.8–3	0.4–0.71	5–8
257.2	0.5–1.5	128	2–10	0.8–3	0.4–0.8	5–8

Note: U: voltage added to the target; I: current; d: distance of target to nozzle (mm); D: diameter of the pore opening size of the nozzle; $\boldsymbol{P}_1$: He (+Ar) pressure in magnetron; P_2: pressure in flow-tube; ν: flow velocity of He-gas.

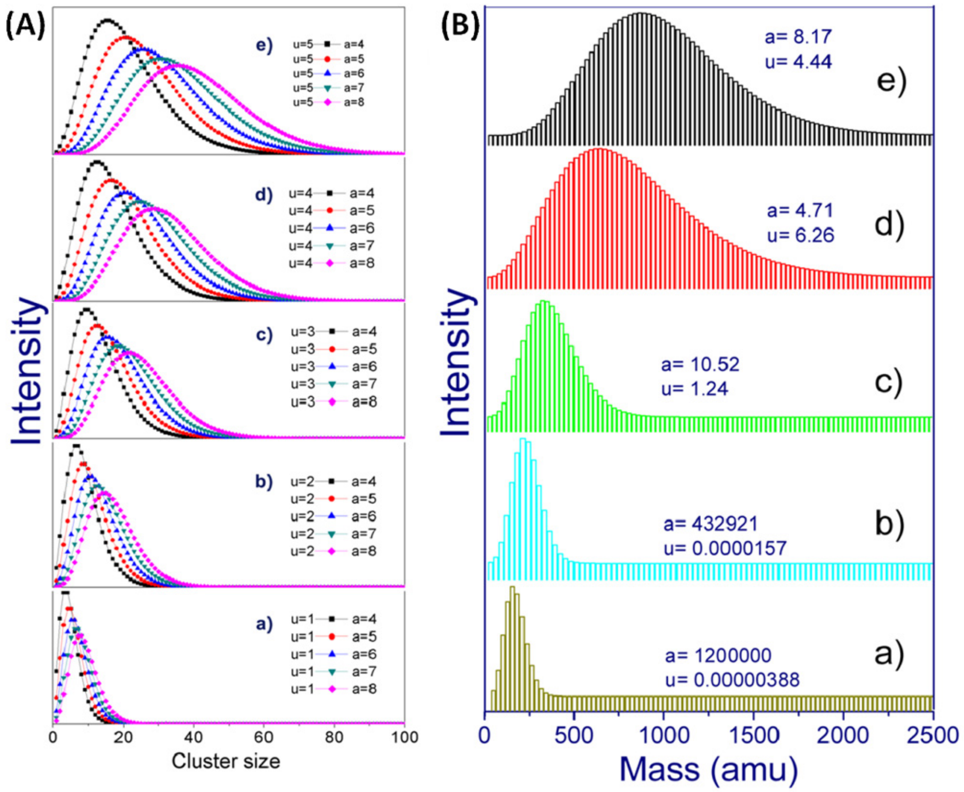

Fig. 6. (A) Population of the cluster ions were calculated according to the distribution function analytically solved from the extended Smoluchowshi rate equation. The various curves correspond to different values of the parameters, *a* and *u*, respectively. (B) The fitting curves for the strength of integral on all the clusters observed in Fig. 5.

can be included in the collision probability (i.e., pressures in the MagS-source).

Further results show that for a certain *a*-value, the size distribution can also be tunable with changes of *u*-values, which indicates that the above correlations are applicable to neutral or ionic cluster distributions equally, and controlling these parameters can be used to modify each distribution separately. This is important when Table 1 is again considered; because it suggests that the adjustability of the MagS-source, which is utilized to tune the cluster distribution and therefore *a*- and *u*-values, is actually modifying the rates of reaction described in Eqs. (2) and (3). In reality, it is likely that the Al clusters from the MagS-source follow physical (inelastic collisions) and chemical (charge-transfer-involved reactions) growth processes. For a physical growing process, the dominant parameters include the local pressures, density of clusters, saturation level and temperature-dependent thermal motion and diffusion, etc.; while a chemical growing process not only involves all these parameters, but also opens up opportunities for the contributions of initial chemical reactions which can be simply a class of electron-transfer reactions.

In the current example, the presence and behavior of electrons in front of the target should provide important contributions to cluster growth. This can be confirmed by the dependence of the size-distribution on the cathode voltage as mentioned above. Calculations also indicate that the *a*-values for the cases of $a > 2$ come to fit better with the experimental results (Fig. 5), which confirms a dominant growth mechanism on ionic Al clusters from the MagS-source. Nevertheless, it is worth mentioning that the proposed aggregation model does not account for the bimodality of the distribution found in some of the experiments (e.g., Figs. 2d–f and 4b), and the fitting parameters for the strength of integral by mathematics are not always satisfied in an exact accordance with the experimental observation, as shown in Fig. 6B. This is because, for simple consideration, the disaggregation of the clusters which might also play any role in the experiments has been neglected. A relatively rigorous consideration of the growth dynamics of cluster populations can be treated as the following equation [16]:

$$\frac{dq_n}{dt} = \sum\nolimits_m q_n P_{m\to n} - q_n \sum\nolimits_m P_{n\to m} \tag{5}$$

where $P_{m\to n}$ is the mean rate at which a cluster *m* converts into an cluster *n*, and a critical cluster size is postulated to be stable if the rate of condensation onto that cluster exceeds the rate of evaporation from it. Based on this theory, the transition processes could be assumed to be Markovian, so that the rate coefficients depend on the properties of the clusters and their real-time environment. Assuming the only important transitions are those involving the addition or loss of single units to or from the cluster, Eq. (5) can further reduce to [16],

$$\frac{dq_n}{dt} = \beta_{n-1} q_{n-1} - \gamma_i q_n - \beta_n q_n + \gamma_{n+1} q_{n+1} \tag{6}$$

where the $\beta_n = P_{n\to n+1}$ and $\gamma_n = P_{n\to n-1}$ refer to the non-zero rate coefficients. This theory suggested the possible existence of Al_n cluster dimers (or trimers) which interact with each other and directly birth a bigger cluster, also possibility for big clusters to become small by fission or crash.

4. Conclusions

Employing a MagS system, we obtained Al clusters with a flexible size distribution which was well controlled via parameter s of the MagS-source. Based on these factors, the growth kinetics of Al clusters was systematically studied by further adjusting the He and Ar pressures, cathode voltages, and the distance from the target to the nozzle, etc. With a verification of fitting curves based on the extended Smoluchowski rate equation, we provide a general interpretation on principles of the growth kinetics of Al clusters in the MagS-source. The agreement of calculations with experimental observation also provides a general protocol for studying cluster growth mechanism in gas-phase.

Acknowledgments

The authors thank K. Don Dasitha Gunaratne for friendly discussion. This work is supported by Air Force Office of Scientific Research through grant FA 9550-10-1-0071.

References

[1] H. Haberland, Clusters of Atoms and Molecules, Springer, Berlin, 1994.
[2] S.N. Khanna, A.W. Castleman Jr., Quantum Phenomena in Clusters and Nanostructures, Springer, Berlin, 2003.
[3] P. Jena, S.N. Khanna, B.K. Rao, Physics and Chemistry of Small Metal Clusters, Plenum, New York, 1987.
[4] A.W. Castleman Jr., R.G. Keesee, Chem. Rev. 86 (1986) 589–618.
[5] A.W. Castleman Jr., R.G. Keesee, Science 241 (1988) 36–42.
[6] S. Sugano, Microcluster Physics, Springer, Berlin, 1991.
[7] A.W. Castleman Jr., R.G. Keesee, Acc. Chem. Res. 19 (1986) 413–419.
[8] A.W. Castleman Jr., I.N. Tang, J. Chem. Phys. 57 (1972) 3629.
[9] A.W. Castleman Jr., P.M. Holland, R.G. Keesee, J. Chem. Phys. 68 (1978) 1760.
[10] R.G. Keesee, N. Lee, A.W. Castleman Jr., J. Am. Chem. Soc. 101 (1979) 2599.
[11] S.F. Cartier, Z.Y. Chen, G.J. Walder, C.R. Sleppy, A.W. Castleman Jr., Science 260 (1993) 195.
[12] J. Wedekind, G. Chkonia, J. Wölk, R. Strey, D. Reguera, J. Chem. Phys. 131 (2009) 114506.
[13] H. Hettema, J.S. McFeater, J. Chem. Phys. 105 (1996) 2816.
[14] A.V. Gusarov, V.I. Titov, I. Smurov, Appl. Surf. Sci. 253 (2007) 7672.
[15] M. Villarica, M.J. Casey, J. Goodisman, J. Chaiken, J. Chem. Phys. 98 (6) (1993) 4610.
[16] I.J. Ford, Inst. Proc. Eng. Mech. Part C: J. Mech. Eng. Sci. 218 (2004) 883–899.
[17] H.L. Jaeger, E.J. Willson, P.G. Hill, K.C. Russell, J. Chem. Phys. 51 (1969) 5380.
[18] J.M. Soler, N. Garcıa, O. Echt, K. Sattler, E. Recknagel, Phys. Rev. Lett. 49 (1982) 1857.
[19] T.P. Martin, T. Bergmann, N. Malinowski, J. Chem. Soc., Faraday Trans. 86 (1990) 2489.
[20] P. Feiden, J. Leygnier, P. Cahuzac, C. Brechignac, Chem. Phys. Lett. 432 (2006) 230.
[21] T.D.d.l Rubia, G. Gilmer, Nat. Mater. 1 (2002) 89–90.
[22] S. Rives, A. Catherinot, F. Dumas-Bouchiat, C. Champeaux, A. Videcoq, R. Ferrando, Phys. Rev. B 77 (2008) 085407.
[23] P.R.t. Wolde, D. Frenkel, J. Chem. Phys. 109 (1998) 9901.
[24] J. Wedekind, D. Reguera, J. Chem. Phys. 127 (2007) 154516.
[25] A. Nakajima, T. Sugioka, K. Hoshino, K. Kaya, Chem. Phys. Lett. 189 (1992) 455.
[26] W.A. deHeer, Rev. Mod. Phys. 65 (1993) 611.
[27] R.S. Bowles, J.J. Kolstad, J.M. Calo, R.P. Andres, Surf. Sci. 106 (1981) 117.
[28] F. Frank, W. Schulze, B. Tesche, J. Urban, B. Winter, Surf. Sci. 156 (1985) 90.
[29] T.P. Martin, J. Chem. Phys. 81 (1984) 4426.
[30] D.E. Powers, S.G. Hansen, M.E. Geusic, A.C. Pulu, J.B. Hopkins, T.G. Dirtz, M.A. Duncan, P.R.R. Langridge-Smith, R.E. Smalley, J. Phys. Chem. 86 (1982) 2556.
[31] S.J. Riley, E.K. Parks, C.R. Mao, L.G. Pobo, S. Wexler, J. Phys. Chem. 86 (1982) 3911.
[32] A. Yokozeki, G.D. Stein, J. Appl. Phys. 49 (1978) 2224.
[33] A. Herrman, S. Leutwyler, E. Schumacher, H.L. Woeste, Chim Acta 61 (1978) 453.
[34] T.G. Dietz, M.A. Duncan, D.E. Powers, R.E. Smalley, J. Chem. Phys. 74 (1981) 6511.
[35] M.M. Kappes, R.W. Kunz, E. Schumacher, Chem. Phys. Lett. 91 (1982) 413.
[36] A.W. Castleman Jr., K.H. Bowen Jr., J. Phys. Chem. 100 (1996) 12911–12944.
[37] U. Heiz, A. Vayloyan, E. Schumacher, Rev. Sci. Instrum. 68 (1997) 3718.
[38] C. Xirouchaki, R.E. Palmer, Phil. Trans. R. Soc. Lond. A 362 (2004) 117–124.
[39] S.J. Carroll, P.D. Nellist, R.E. Palmer, S. Hobday, R. Smith, Phys. Rev. Lett. 84 (2000) 2654.
[40] R.E. Palmer, S. Pratontep, H.-G. Boyen, Nature Mater. 2 (2003) 443.
[41] B. Wortmann, K. Mende, S. Duffe, N. Grönhagen, B.v. Issendorff, H. Hövel, Phys. Status Solidi B 247 (2010) 1116.
[42] B. Windows, N. Savvides, J. Vac. Sci. Technol. A 4 (3) (1986) 453.
[43] H. Haberland, M. Mall, M. Mosler, Y. Qiang, T. Reiners, Y. Thumer, J. Vac. Sci. Technol. A 12 (5) (1994) 2925.
[44] P.J. Kelly, R.D. Arnell, Vacuum 56 (2000) 159.
[45] M.v. Smoluchowski, Z. Phys. Chem. 92 (1917) 129.
[46] M.v. Smoluchowski, Phys. Z. 17 (1916) 557.
[47] D.E. Bergeron, P.J. Roach, A.W. Castleman, N. Jones, S.N. Khanna, Science 307 (2005) 231–235.
[48] A.W. Castleman Jr., K.G. Weil, S.W. Sigsworth, R.E. Leuchtner, R.G. Keesee, J. Chem. Phys. 86 (1987) 3829.
[49] P.J. Roach, W.H. Woodward, A.W. Castleman Jr., A.C. Reber, S.N. Khanna, Science 323 (2009) 492–495.
[50] S. Pratontep, S.J. Carroll, C. Xirouchaki, M. Streun, R.E. Palmer, Rev. Sci. Instrum. 76 (2005) 045103.
[51] R. Morel, A. Brenac, P. Bayle-Guillemaud, C. Portemont, F.L. Rizza, Eur. Phys. J. D 24 (2003) 287–290.
[52] C.G. Granqvist, R.A. Buhrman, J. Appl. Phys. 47 (1976) 2200–2219.
[53] J.Y. Rempel, M.G. Bawendi, K.F. Jensen, J. Am. Chem. Soc. 131 (2009) 4479.
[54] R.B. Huang, Q. Zhang, H. Chen, L.S. Zheng, Eur. Phys. J. D 9 (1999) 253.